Eco. Env. & Cons. 30 (January Suppl. Issue) : 2024; pp. (S395-S400)
Copyright@ EM International
ISSN 0971–765X

DOI No.: http://doi.org/10.53550/EEC.2024.v30i01s.079

Solar Light Driven Photocatalytic Activity of TiO_2 Coupled Bi_2O_4 Nanocomposites

T. Vimala[1,2], A. Sivarajan[1]*, T. Rajachandrasekar[3] and K. Veeravelan[3]

[1]Department of Chemistry, Govt. Arts College, Tiruchirappalli 620 022, (Affiliated to Bharathidasan University), Thiruchirappalli- 24)Tamilnadu, India
[2]Department of Chemistry, S.T.E.T. Women's College (Autonomous) (Affiliated to Bharathidasan University, Thiruchirappalli- 24), Mannargudi 614 016, Tamilnadu, India
[3]Photocatalysis Laboratory, Department of Chemistry, M.R. Govt. Arts College, Mannargudi 614 001(Affiliated to Bharathidasan University, Thiruchirappalli- 24), Tamilnadu, India

(Received 20 August, 2023; Accepted 16 October, 2023)

ABSTRACT

TiO_2/Bi_2O_4 nano composite photocatalyst was synthesized by sol-gel method. The chemical composition morphology and micro structural features of the materials were characterized by Fourier transform infrared (FT-IR) spectroscopy, X-ray diffraction (XRD) analysis, scanning electron microscopy (SEM) with energy dispersive X-ray (EDX) analysis and UV-vis-diffuse reflectance spectroscopy (UV-vis-DRS). The synthesized nano composite were used as photocatalyst materials for the degradation of Eosin Yellow (EY) dye under solar light irradiation. The effect of pH and reusability were studied. The mechanism of photocatalytic degradation also discussed.

Key words: *Eyosin Yellow, Nanocomposite, Photocatalytic degradation, TiO_2 / Bi_2O_4*

Introduction

Dyes, in particular azo dyes, are the major by-product of the textile industry dyes have been used to color textiles in order to provide a variety of fabrics to choose from, but at the cost of polluting the environment. It has been estimated by the World Health Organization (WHO) that 17-20% of industrial water pollution is caused by the dying treatment of textiles, while about 80% of the dying process is done using azo dyes. Azo dyes are known to have acute carcinogenic effects to human and a negative impact on the environment. Hence it is becoming a global urgency to mitigate this issue (Hasan *et al*., 2021). The semiconductor-assisted photocatalysis process has proven to be effective for the decomposition of organic pollutants. Such as acids, dyes and aromatic and phenolic compounds, etc., (Gowthami *et al.,* 2018) which are present in wastewater, due to its strong redox potential, environment friendliness, (Gowthami *et al.,* 2020) moderate operation temperature, easy operation and useful final products (Muthuvel *et al.,* 2014). Nano structured semiconductors show great potential for environmental remediation because of photocatalytic oxidation, (Hu, *et al.,* 2017) which is activated under the solar light or UV light (Liu, *et al.,* 2015). This has prompted the scientific community to effectively develop elimination technologies, which are known as advanced oxidation processes (AOPs) (Feizpoor, *et al*., 2018). These processes are based on the production of hydroxyl radicals which are strong oxidizing agents for mineralizing organic pollutants. Among the various AOPs attention has been paid to

semi-conductor photocatalysts (*e.g.* TiO_2) (M'Bra, *et al.*, 2019). By far the most researched photocatalytic material is anatase TiO_2 because of its long-term thermodynamic stability. Strong oxidizing power, low cost and relative non toxicity (Tan, *et al.*, 2013). However, the rapid recombination of electrons and holes is one of the main reasons for the low photocatalytic efficiency of TiO_2. (Alizadeh, *et al.*, 2019) Moreover its wide band gap of 3.2 eV (Cheng, *et al.*, 2018). Recently, a new visible-light-driven photocatalytic of Bi_2O_4 was synthesized and used to photodegrade organic contaminants (Hameed, *et al.*, 2015). It is a simple oxide with a narrow band gap (~2.0 eV) and a mixed valence of Bi^{3+} and Bi^{5+}, exhibiting better photocatalytic activity than other visible light catalysts such as CdS and Bi_2O_3 (Xia, *et al.*, 2017). Therefore, in this study, we have design the Bi_2O_4 modificated TiO_2 heterojunction photocatalyst by the sol-gel method. The photocatalytic activity of the TiO_2/Bi_2O_4 nano composite under solar-light irradiation was explored by using Eyosin Yellow (EY) dye. In addition, a possible mechanism for degradation was also proposed.

Experimental

Materials

The commercial Eosin Yellow (EY) dye (C.I. No. 45380), Titanium isopropoxide, isopropanol (AVRA Chemicals), sodium bismuthate (Hi-Media) were used as received. The experimental solution was prepared using distilled water.

Methods

Fabrication of the TiO_2/Bi_2O_4 Catalyst

Sodium bismuthate ($NaBiO_3.2H_2O$) was dispersed in deionized water (60 ml) and stirred at room temperature for 10 min to form a suspension. The resulting suspension was loaded into a Teflon-linked stainless steel autoclave with a capacity of 100 ml and maintained at 160°C for 12 h. After cooling, the resultant product was washed three times with described water and ethanol and then dried overnight in an oven at 60°C. 19 wt% of Bi_2O_4 was mixed with an appropriate amount of titanium isopropoxide (12.5 ml) and isopropanol (80 ml) solution. The mixed suspension is stirred for 6 h. The precipitate was filtered, washed with deionized water several times, and dried in a hot air oven at 80 °C for 6 h. A TiO_2-Bi_2O_4-coupled system is taken in a silica crucible and calcined at 450 °C for 12 h in a muffle furnace at the rate of temperature increase of 20 °C min^{-1}. After 12 h, the furnace is allowed to cool down to room temperature. The TiO_2/Bi_2O_4 catalyst is collected and used for further analysis. This catalyst has 19 wt% Bi_2O_4 and catalyst. Similarly, 13, 16, and 21 wt% of Bi_2O_4-coupled TiO_2 are prepared using an appropriate amount of Bi_2O_4. The bare TiO_2 catalyst is prepared using this procedure without Bi_2O_4. Photocatalytic Degradation Experiments and Characterization Techniques are reported earlier (Gowthami, *et al.*, 2020)

Results and Discussion

FT-IR and XRD analysis

The FT-IR spectra of the prepared TiO_2, Bi_2O_4 and TiO_2/Bi_2O_4nanocatalyst are shown in Figure 1. The OH stretching vibrations are observed in the range of 3421-3417 cm^{-1} for all the samples. In Figure 1a, the absorption bands at 600-400 cm^{-1} are attributed to the Ti--O group, respectively (Feizpoor, *et al.*, 2018). In Figure 1b the band located at 414 cm^{-1} is corresponded to the Bi–O vibration (Khazaee, *et al.*, 2019). Figure 1c show that both Ti-O and Bi–O stretching vibration are observed in the range of 600-400 cm^{-1}. The obtained results provide evidence that Bi_2O_4 is loaded effectively on TiO_2. The crystal structure of TiO_2, Bi_2O_4 and TiO_2/Bi_2O_4 catalysts was studied by powder XRD analysis as shown in Figure 2. The characteristic peaks of TiO_2 at 2θ values of 25.3, 37.7, 47.9 and 54.9° match with (101), (004), (200) and (105) planes of TiO_2 (JCPDS No. 21-1272)

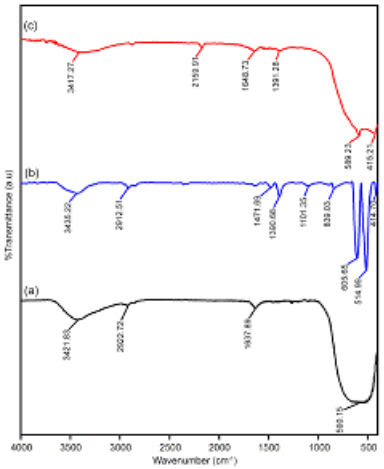

Fig. 1. FT-IR spectra of (a) TiO_2, (b) Bi_2O_4 and (c) TiO_2/Bi_2O_4

(Li, *et al.*, 2017) (Figure 2a). Figure 2b reveals that the rod-like Bi_2O_4 is ascribed to the monoclinic phase of

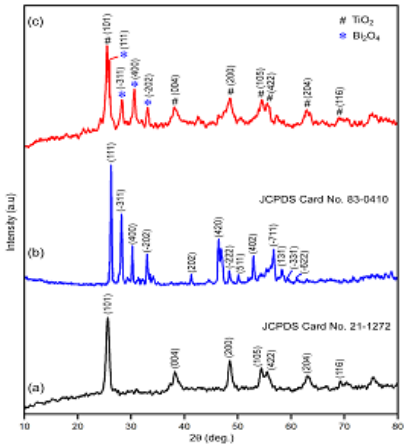

Fig. 2. XRD patterns of (a) TiO_2, (b) Bi_2O_4 and (c) TiO_2/Bi_2O_4

Bi_2O_4 (JCPDS No. 83-0410) (Zhang, *et al.*, 2020) and the intense peaks indicate the samples are well crystallized. Figure 2c shows for all the TiO_2/Bi_2O_4 heterojunctions, monoclinic Bi_2O_4 and anatase TiO_2 peaks can be clearly observed in the XRD patterns confirming that Bi_2O_4 has successfully combined with TiO_2.

SEM-EDX

SEM studies provide useful information regarding the surface morphology of materials. SEM images of 19 wt% TiO_2/Bi_2O_4 at three different magnifications are shown in Figure 3. The magnified SEM image of

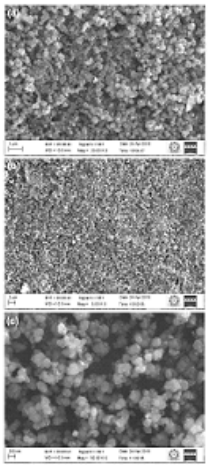

Fig. 3. SEM images of TiO_2/Bi_2O_4 (a) 1 µm, (b) 2 µm and (c) 200 mm

TiO_2/Bi_2O_4 shows that a large number of particles were formed in the cavity or on the surface of hierarchical TiO_2 indicating the morphology of Bi_2O_4 changes from the submicro rod morphology structure with diameter of about 300-500 nm and length of about 2-4 mm. The elemental composition and purity of TiO_2/Bi_2O_4 sample were also analyzed by energy dispersive X-ray (EDX) analysis. Figure 4 shows the EDX spectrum of

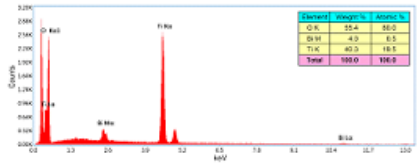

Fig. 4. EDX of TiO_2/Bi_2O_4

TiO_2/Bi_2O_4 sample which shows the presence of Ti, Bi and O by the appearance of Ti, Bi and O peaks without any other characteristic peaks. Hence, the EDX results are perfect evidences to propose that the prepared sample does not contain any other elements and is indeed free from other impurities.

UV-Vis-DRS

To understand the light absorption capacity of the as-prepared photocatalysts, the UV-Vis diffuse reflectance spectra of TiO_2, Bi_2O_4 and TiO_2/Bi_2O_4 are detected (Figure 5A). As we can see that the absorption edge of TiO_2 locates at the UV range, the absorption threshold wavelength of Bi_2O_4 is about 620 nm and strong absorption is observed in the visible light region. Compared to TiO_2, TiO_2/Bi_2O_4 heterostructures have obvious red shift phenomenon, confirming the successful incorporation of Bi_2O_4 into TiO_2. In general, the wider is the visible light response range and higher visible light absorption intensity, the better is the visible light photocatalytic activity of photocatalyst. From the K.M. plot, the band gap energy was estimated at 3.23, 1.97, and 3.19 eV for TiO_2, Bi_2O_4, and TiO_2/Bi_2O_4, respectively (Fig. 5B).

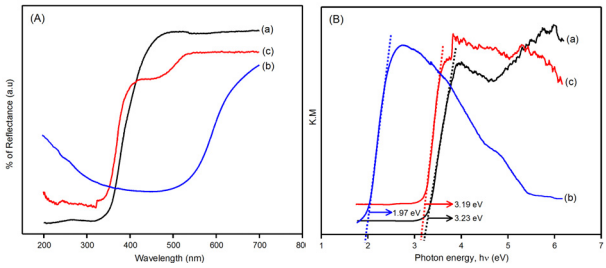

Fig. 5. A) UV-Vis-DRS spectra and B) K.M plot of a) TiO_2, b) Bi_2O_4 and c) TiO_2/Bi_2O_4

Primary analysis

The photocatalytic activities of EY with TiO_2/Bi_2O_4 catalysts using solar light under different conditions are shown in Figure 6. The dye is resistant to direct photolysis by solar light (curve a). There is a small decrease in concentration of dye observed when it is

treated with TiO_2/dark for 90 min (curve b). When the dye was put on irradiation with TiO_2 under solar light, 54% percentage of degradation was observed at 90 min (curve c). A small decrease in dye concentration (27%) occurred when it was treated with dye/TiO_2/Bi_2O_4/dark (curve f) for 90 min. The degradation of dye on irradiation with TiO_2/Bi_2O_4 catalyst of different wt% of Bi_2O_4 is shown in curves d, e, g, and h, and catalyst with 19 wt% TiO_2/Bi_2O_4 shows a higher degradation (curve g, 91%). Hence, 19 wt% of Bi_2O_4 is taken as optimum concentration of Bi_2O_4 on TiO_2 for further studies.

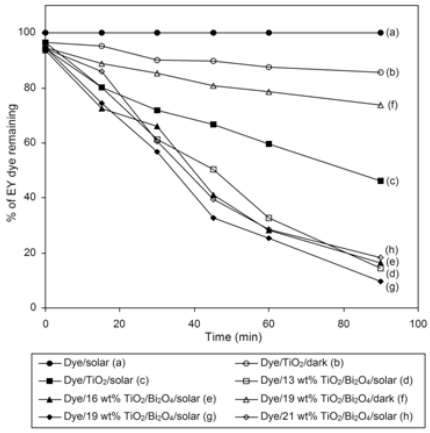

Fig. 6. Primary analysis of TiO_2/Bi_2O_4 catalyst with EY dye under solar light
[EY] = 1 × 10^{-4} M, 19 wt%TiO_2/Bi_2O_4 = 2 g L^{-1}, airflow rate = 8.1 mL s^{-1}, pH = 6.0, I_{solar} = 1250 ×100 ± 100 lux

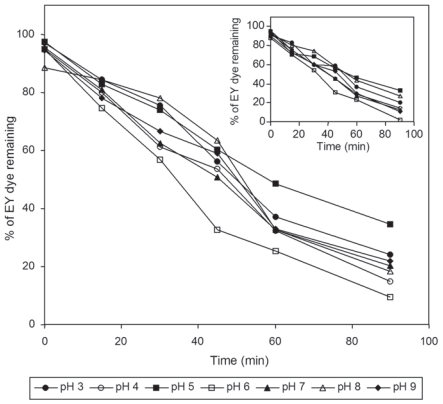

Fig. 7. Effect of pH (degradation).
[EY] = 1 × 10^{-4} M,
19 wt% TiO_2/Bi_2O_4 = 2 gL^{-1}
airflow rate = 8.1 mL s^{-1},
I_{solar} = 1250 × 100 ± 100 lux.
Inset shows effect of pH (decolorization)

Effect of pH

The effect of pH value of solution on the degradation and decolorization of EY was studied in the range of 3-9 and the results were shown in Figure 7. The percentage of degradation (76 to 95%) and decolorization (80 to 98%) was found to increase with an increase of pH from 3 to 6 at 90 min. As it was expected, the complete degradation and decolorization was achieved in the investigated pH range at the optimum pH of 6. Further increase in pH above 6 causes the percentage of degradation and decolorization to decrease. Above pH 6 this value the TiO_2/Bi_2O_4 surface is negatively charged. It is expected that at pH 6, there is a strong interaction between negatively charged catalyst and dye cation consequently (Muthuvel *et al.*, 2020). The optimum pH is 6.

Reusability

Estimating the stability and reusability of photocatalytic is indispensable for the practical application of TiO_2/Bi_2O_4. The dye concentration of EY was kept constant at 1×10^{-4} M and was exposed to solar light irradiation 120 min for each cycle. The catalyst dosage of photocatalyst was 2 g l^{-1}. The photocatalyst was recycled after filtrating and heating treatment at 100 °C for 8 h for every cycle. The results are shown in Figure 10. The degradation efficiency of the catalyst in all the five runs is 1st run to 3rd runs 93, 93, 93%, 4th and 5th runs 98 and 98% degradation at 120 min.

Mechanism

A possible mechanism involved in the formation of TiO_2/Bi_2O_4nanocomposite is predicted from Figure 11. Considering the band positions, the conduction band (CB) and valence band (VB) of Bi_2O_4 were

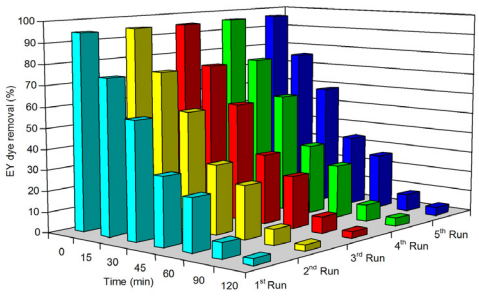

Fig. 10. Reusability. [EY] = 1 ´ 10^{-4} M, 19 wt% TiO_2/Bi_2O_4 = 2 g L^{-1}, airflow rate = 8.1 mL s^{-1}, pH = 6.0, irradiation time = 120 min, I_{solar} = 1250 × 100 ± 100 lux

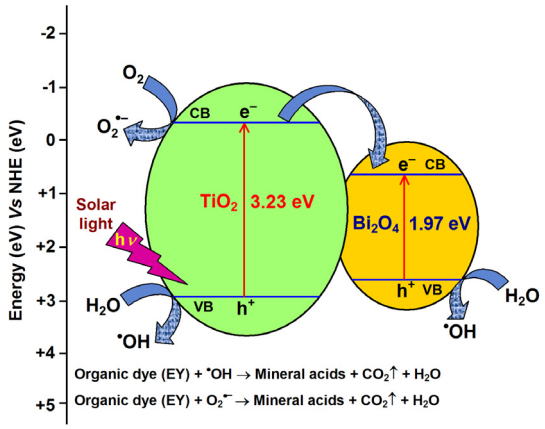

Fig. 11. Schematic representation of formation of TiO_2/Bi_2O_4 heterojunction for EY dye degradation

found at +0.649 and +2.619 eV, respectively and those of TiO_2 were observed at –0.335 and +2.895 eV, respectively. The appropriate band positions of TiO_2 and Bi_2O_4 promote the formation of the heterojunction structure and enhance the photocatalytic activity. Under light irradiation, the photoexcited electrons in the CB of TiO_2 can jump to the CB of Bi_2O_4. The CB potential of Bi_2O_4 was found to be more electronegative than the reduction potential of $O_2/O_2^{\cdot-}$ (–0.34 eV *Vs*NHE), and therefore the electrons concentrated in the CB of Bi_2O_4 can generate $O_2^{\cdot-}$ for dye degradation. Meanwhile the holes on the VB bands of TiO_2 and Bi_2O_4 oxidize H_2O- to produce $^{\cdot}OH$, and it is a highly oxidative species towards dye degradation. The band gap energy obtained by Kubelka-Munk (KM) function is comparatively lower than pure undoped TiO_2.

Conclusion

Nanocomposites of TiO_2/Bi_2O_4 synthesized by sol-gel method. The nanocomposite characterized by FT-IR, XRD, SEM-EDX and UV-Vis-DRS analysis. Photocatalytic decomposition of EY was analysed with different pHs and reusability. Analysis of the reusability of the catalyst revealed that the catalyst is stable and reusable. A suitable degradation mechanism was also proposed.

References

Alizadeh, S., Fallah, N. and Nikazar, M. 2019. An ultrasonic method for the synthesis, control and optimization of CdS/TiO_2 core-shell nanocomposites. *RSC Advances.* 9: 4314-4324.

Cheng, J., Wang, X., Zhang, Z., Shen, Y., Chen, K., Guo, Y., Zhou, X. and Bai, R. 2018 Synthesis of flower-like Bi_2O_4/ZnOheterojunction and mechanism of enhanced photodegradation for organic contaminants under visible light. *Research on Chemical Intermediates.* 44: 6569-6590.

Feizpoor, S. and Habibi-Yangjeh, A. 2018. Ternary TiO_2/Fe_3O_4/$CoWO_4$ nanocomposites: Novel magnetic visible-light-driven photocatalysts with substantially enhanced activity through p-n heterojunction. *Journal of Colloid and Interface Science*. 524: 325-336.

Feizpoor, S., Habibi-Yangjeh, A. and Yubuta, K. 2018. Integration of carbon dots and polyaniline with TiO_2 nanoparticles: substantially enhanced photocatalytic activity to removal various pollutants under visible light. *Journal of Photochemistry and Photobiology A: Chemistry*. 367: 94-104.

Gowthami, K., Suppuraj, P., Thirunarayanan, G., Krishnakumar, B., Sobral, A.J.F.N., Swaminathan, M. and Muthuvel, I. 2018. $Fe_2V_4O_{13}$ assisted hetero-Fenton mineralization of methyl orange under UV-A light irradiation. *Iranian Chemical Communication.* 6: 97-108.

Gowthami, K., Krishnakumar, B., Thirunarayanan, G., Swaminathan, M. and Muthuvel, I. 2020. Novel $Fe_2V_4O_{13}$/ZnO nano-heterojunction: Effective decomposition of methyl orange under solar light irradiation. *Materials Today: Proceedings*. 29: 1199-1203.

Gowthami, K., Krishnakumar, B., Sobral, A.J.F.N., Thirunarayanan, G., Swaminathan, M., Siranjeevi, R., Rajachandrasekar, T. and Muthuvel, I. 2020. Fabrication of hybrid $Fe_2V_4O_{13}$/ZnO heterostructure for effective mineralization of aqueous methyl orange solution. *Journal of Cluster Science.* 31: 839-849.

Hasan, N., Dalayoan, D.J., Lee, J., Lee, J., Kim, J., Bae, J.S. and Liu, C. 2021 Ag^0/Au^0 nanocluster loaded Bi_2O_4 photocatalyst for methyl orange dye photodegradation. *RSC Advances.* 11: 26607-26619.

Hameed, A., Aslam, M., Ismail, I. M., Salah, N. and Fornasiero, P. 2015. Sunlight induced formation of surface Bi_2O_{4-x}–Bi_2O_3nanocomposite during the photocatalytic mineralization of 2-chloro and 2-nitrophenol. *Applied Catalysis B: Environmental*. 163: 444-451.

Hu, J., Chen, D., Li, N., Xu, Q., Li, H., He, J. and Lu, J. 2017. *In situ* fabrication of $Bi_2O_2CO_3$/MoS_2 on carbon nanofibers for efficient photocatalytic removal of NO under visible-light irradiation. *Applied Catalysis B: Environmental.* 217: 224-231.

Khazaee, Z., Mahjoub, A.R., Khavar, A.H.C., Srivastava, V. and Sillanpää, M. 2019. Synthesis of layered perovskite Ag, F-Bi_2MoO_6/rGO: A surface plasmon resonance and oxygen vacancy promoted nanocomposite as a visible-light photocatalyst. *Journal of Photochemistry and Photobiology A: Chemistry*. 379: 130-143.

Muthuvel, I., Krishnakumar, B. and Swaminathan, M. 2014. UV-A/solar light induced Fenton mineralization of Acid Red 1 using Fe modified bentonite composite. *Indian Journal of Chemistry.* 53A: 672-678.

Li, X., Zhang, C., Hu, C., Xu, L., Hu, Q., Duo, S., Li, W. and Kang, Y. 2017. Synthesis of Bi_2O_4@TiO_2 heterojunction with enhanced visible light photocatalytic activity. *Journal of Cluster Science.* 28: 2409-2418.

Liu, J., Liu, Y., Liu, N., Han, Y., Zhang, X., Huang, H., Lifshitz, Y., Lee, S.T., Zhong, J. and Kang, Z. 2015. Metal-free efficient photocatalyst for stable visible water splitting via a two-electron pathway. *Science.* 347: 970-974.

M'Bra, I.C., Atheba, G.P., Robert, D., Drogui, P. and Trokourey, A. 2019. Photocatalytic degradation of paraquat herbicide using a fixed bed reactor containing TiO_2 nanoparticles coated onto b-SiC alveolar foams. *American Journal of Analytical Chemistry*. 10: 171-184.

Muthuvel, I., Gowthami, K., Thirunarayanan, G., Krishnakumar, B., Swaminathan, M. and Siranjeevi, R. 2020. Solar light-driven $CeVO_4$/ZnO nanoheterojunction for the mineralization of Reactive Orange 4. *Environmental Science and Pollution Research*. 27: 43262-43273.

Tan, L.L., Ong, W.J., Chai, S.P. and Mohamed, A.R. 2013. Reduced graphene oxide-TiO_2nanocomposite as a promising visible-light-active photocatalyst for the conversion of carbon dioxide. *Nanoscale Research Letters.* 8: 1-9.

Xia, D., Wang, W., Yin, R., Jiang, Z., An, T., Li, G., Zhao, H. and Wong, P.K. 2017. Enhanced photocatalytic inactivation of *Escherichia coli* by a novel Z-scheme g-C_3N_4/ m-Bi_2O_4 hybrid photocatalyst under visible light: the role of reactive oxygen species. *Applied Catalysis B: Environmental*. 214: 23-33.

Zhang, C., Ma, Y., Li, C., Qin, F., Hu, C., Hu, Q. and Duo, S. 2020. Spatially confined growth of Bi_2O_4 into hierarchical TiO_2 spheres for improved visible light photocatalytic activity. *Journal of Materials Science.* 55: 3181-3194.